Title: Soil-geosynthetic interaction in pullout and inclined-plane shear for two geosynthetics exhumed after installation damage

Authors: M. Pinho-Lopes[*1], A.M. Paula[2] and M.L. Lopes[3]

[1] Lecturer, Faculty of Engineering and the Environment, University of Southampton, Highfield, Southampton SO17 1BJ, United Kingdom, Telephone: +44 (0)2380598363; Fax: +442380677519; Email: M.Pinho-Lopes@sonton.ac.uk

[2] Adjunct Professor, Department of Applied Mechanics, Polytechnic Institute of Bragança, Campus de Santa Apolónia, 5300-253 Bragança, Portugal, Telephone: +351 273 303 154; Fax: +351 273 325 405; E-mail: mpaula@ipb.pt

[3] Full Professor, Department of Civil Engineering, Faculty of Engineering, University of Porto, Rua Dr. Roberto Frias, s/n 4200-465 Porto Portugal, Telephone: +3515081564; Fax: +3515081446; E-mail: lcosta@fe.up.pt

[*] Corresponding author

Abstract:

This paper contributes to better understanding how installation damage of geosynthetics can affect the soil-geosynthetic interaction on pullout and inclined-plane shear. The effects of installation damage induced in field trials of a woven geotextile and a woven geogrid were studied. The results indicated that after installation the accumulation of a layer of fine particles over the geosynthetics can reduce the skin friction available, particularly for sheet materials. Installation damage can induce premature tensile failures in pullout tests, along the unconfined section of geosynthetics, causing a significant reduction of the corresponding coefficient of interaction. The contribution of the bearing members to the coefficient of interaction in pullout was estimated using equations from the literature. Such estimates were too optimistic. The installation damage induced had little influence on the soil-geosynthetic coefficient of interaction in inclined plane shear. The different relative movements of soil and geosynthetic in pullout and inclined-plane shear, as well as the deformation of the reinforcements during pullout, enabled different mobilisation of the interface strength. For the comparable conditions tested, the coefficient of interaction from inclined plane shear tests was larger than that measured from pullout tests. The reduction factor for installation damage obtained from tensile tests overestimated the effects of the installation conditions on the soil-geosynthetic interface from both pullout and inclined plane shear tests.

Keywords:
Geosynthetics, installation damage, coefficient of interaction, pullout, inclined plane shear

1 INTRODUCTION

For reinforced soil applications, usually geosynthetics are installed between compacted layers of coarse backfill material. The construction and installation processes induce actions that are likely to provoke mechanical damage, which in turn can affect the performance of the reinforcements. It is generally accepted that installation damage of geosynthetics can affect the hydraulic properties of the materials and originate tensile strength reductions. This paper addresses the influence of construction and installation processes under real conditions on the soil-geosynthetic interface strength in pullout and inclined-plane shear movements.

According to Greenwood et al. (2012), it may be possible to quantify the reduction in strength of reinforcing geosynthetics by measuring it, assuming that the mechanical loads in service are much less than those during the short period of installation and that they cause insignificant damage. Thus, for reinforcement applications most design codes make use of a reduction factor for installation damage (RF_{ID}) expressing the losses in tensile strength after installation and defined as the ratio between the tensile strength of the intact material and that of the material after installation. Nevertheless, different strategies have been used to account for the mechanical damage of geosynthetics in their design. Some countries have produced guidance documents or specifications (such as AASHTO (2011) M288-06, in the USA, and FGSV (2005), in Germany), based on survivability from installation stresses. However, often these do not apply to reinforcements. Alternative approaches include performing installation trials and assessing the changes in tensile properties and deriving installation damage reduction factors (eg., Hufenus et al. 2005; Lim and McCartney 2013; Pinho-Lopes and Lopes 2013). In the absence of relevant data, some guides (for example, EN ISO/TR 20342 (BSI 2007)) recommend using interpolations, either for the same geosynthetic using measurements with different soils, or for other products within the same product line. Databases of test results have been analysed statistically to carry out reliability analysis for installation damage (Bathurst et al. 2011, Miyata and Bathurst 2015).

The degree of mechanical damage depends on the geosynthetic (structure and constituent type), the backfill soil (grain size, angularity and lifts), the method of installation (procedures and construction equipment) and the climatic conditions (Austin 1998, Watn and Chew, 2002, Hufenus et al. 2005). The influence of installation damage on the in-isolation mechanical properties of geosynthetics has been studied extensively. For example, Allen and

Bathurst (1994), Hufenus et al. (2005), Huang and Chiou (2006), Huang and Wang (2007), Pinho-Lopes and Lopes (2013) focused on the short-term response of geosynthetics, while Allen and Bathurst (1996), Greenwood (2002), Cho et al. (2006) and Bathurst and Miyata (2015) analysed their long-term behaviour. Pinho-Lopes et al. (2015) studied the effect of installation damage on the strength of soil-geogrids interface during pullout.

Reinforced soil systems rely on the effectiveness of the transference of tensile stresses from soil to the reinforcements, which, in turn, highly depend on the soil-geosynthetic interaction mechanisms and properties (Lopes 2012). Depending on the region of a reinforced soil structure and the loading conditions, different failure or deformation mechanisms can occur. Palmeira (2009) identified some tests which, although limited, can help analysing such interaction mechanisms: direct shear, in-soil plane strain and pullout tests. In slopes, such as for linings in cover systems of waste disposal areas or erosion control systems, the inclined plane shear test is often used to characterise the soil-geosynthetic interaction under low normal stresses (Palmeira et al. 2002), as in this type of applications the confining stress usually corresponds to a soil height up to 1.00m (Lopes 2013).

During pullout there is relative movement between the geosynthetic and the soil, which leads to the mobilisation of skin friction along the reinforcement and, for grid type reinforcements, soil-soil friction on their openings and passive thrust on their bearing members. The behaviour of the soil-geosynthetic interface in pullout depends on: particle size distribution and density of the soil; structure of the geosynthetic; ratio between the geogrid apertures and the soil grain sizes, when relevant (Lopes and Ladeira 1996, Lopes and Lopes 1999a). Increasing the soil density leads to increasing interface strength in pullout. Pullout failures tend to occur at low confining stresses, in the upper sections of reinforced soil structures. For higher confining stresses failures are usual in tensile or direct shear. Recently several authors have studied the pullout response of soil-geosynthetic interfaces using laboratory tests (Abdi and Zandieh (2014), Ezzein and Bathurst (2014), Lajevardi et al. (2014), Pinho-Lopes et al. (2015)), numerical simulations (Tran et al. (2013), Wang et al. (2014)) and combinations of laboratory tests, numerical simulations and/or analytical approaches (Weerasekara and Wijewickreme (2010), Zhou et al. (2012), Chen et al. (2014), Huang et al. (2014)). During pullout of extensible reinforcements (such as geosynthetics), the friction develops progressively. While the front end of the reinforcement reaches very large strains, its far back end may not be mobilized (Weerasekara and Wijewickreme (2010)). Thus, the pullout response of a confined geosynthetic depends on both the soil-geosynthetic interface behaviour and the stress–strain behaviour of the reinforcement material.

The soil-geosynthetic angle of friction at low normal stress can be determined using an inclined plane apparatus according to EN ISO 12957-2 (BSI 2005), often designated as the "Standard Displacement Procedure". The angle of friction of the soil-geosynthetic interface (δ_{sg}) is determined by from the inclination angle, β_{50}, of the apparatus at which the upper box slides to a displacement of 50 mm. Gourc and Reyes Ramirez (2004) recommend dynamics-based interpretation of the inclined plane shear tests. These authors distinguish three phases for the upper box sliding behaviour: phase 1, a static phase; phase 2, a transitory phase ; phase 3, a non-stabilized-sliding phase. The transitory phase can exhibit a sudden sliding, characterized by an abrupt displacement of the upper box, or gradual sliding, in which the displacement of the upper box increases with the inclination, either progressively or exhibiting a stick-slip mode (Pitanga et al. 2009). Briançon et al. (2011) proposed an alternative method (designated as "force procedure") for determining the soil-geosynthetic angle of friction from inclined-plane shear tests. To apply the method it is necessary to modify significantly the test apparatus. Briançon et al. (2011) reported that the method prescribed in the test standard EN ISO 12957-2 (BSI 2005), overestimated the friction angle of several geosynthetic-geosynthetic interfaces, in particular for gradual sliding.

The soil-geosynthetic interaction is crucial for the response of geosynthetic reinforcements. If installation damage affects the properties of the interface between soil and geosynthetic, namely its strength, the design of reinforced soil structures should allow for that effect. In this paper the soil-geosynthetic interaction response of two geosynthetics was studied using pullout and inclined-plane shear tests, to better understand the changes in response after exhumation from field installation trials. Reduction factors for installation damage were calculated, to contribute to the creation of databases for the design of reinforced soil structures.

2 EXPERIMENTAL PROGRAM

2.1 Test program

The test program presented in this paper included characterising the soil-geosynthetic interface of exhumed geosynthetics after field installation. The soil-geosynthetic interface was characterized in laboratory using pullout and inclined-plane shear tests (Table 1). These tests did not aim to replicate the conditions in the field damage trials, but to assess the influence of the installation damage induced on the soil-geosynthetic interface response. Additionally, to better understand the effects of installation damage on the geosynthetics, scanning electron microscopy images were taken.

The samples of geosynthetics were exhumed after installation in temporary embankments. To realistically represent installation damage, typical procedures for building reinforced soil structures were utilized. The equipment used to spread, level and compact the soil was the same in all the embankments and no construction equipment circulated over the geosynthetics, without a minimum coverage of 0.15m soil.

The embankments (Figure 1) were built in two road constructions sites, using the road platform as a foundation layer (which was free from roots and sharp materials). On that layer a 0.20m lift of soil was spread, levelled and compacted. Then, the geosynthetics were placed, free from wrinkles. Two other soil lifts (0.20m high each) were built sequentially over the geosynthetics. On each construction site a different soil was used, which was compacted using a vibratory roller (Table 2) to two different energies, designated as CE1 and CE2 – necessary to achieve a relative compaction of 90% and 98% of the standard Proctor, respectively. For the compaction control a nuclear densymeter was used, using the standard Proctor of the soil (ASTM 2000, D 698-00a) as a reference. The samples were exhumed using machinery and then manually (Figure 1c), near the geosynthetics.

After the field installation damage different samples were available to be studied (Table 1): exhumed after installation damage (ID) in contact with soil S1 compacted to energy CE1 or CE2; exhumed after installation damage (ID) in contact with soil S2 compacted to energy CE1 or CE2.

The pullout tests (Table 1) were performed with the equipment and procedures described by Pinho-Lopes et al. (2015) and according to BSI (2004) - EN 13738:2004. A large box (Figure 2a) was used (internal dimensions: 1.53m long, 0.90m wide and 0.60m high), equipped with a steel sleeve (0.20m long and 0.48m wide). For the test a capstan clamp was placed inside the sleeve, minimizing the initial unconfined section of the geosynthetics. The initial confined area of the specimens tested was approximately 1.0m long x 0.3m wide and was instrumented with 5 linear potentiometers, to measure internal displacements. A geosynthetic specimen was placed at middle height of the box, between layers of compacted soil (to a relative density I_D=50%). The tests were performed at a displacement rate of 2mm/min using three valid specimens per sample (as defined in BSI (2004) - EN 13738:2004).

The inclined plane shear tests (Table 1) were performed according to BSI (2005), EN ISO 12957-2, using different test methods, depending on the type of geosynthetic: 1) placing the geosynthetic over a rigid metal base (for sheet materials) or 2) using a lower box filled with soil (for geogrids). The specimens were 0.43m wide and 0.70m long. The vertical stress applied was 10kPa. The soil was compacted to a relative density I_D=50%. For each sample three specimens were tested at an inclination rate of 0.5°/min. The equipment (Figure 2b) is further detailed by Lopes et al. (2001). According to the test standard (BSI 2005) the maximum grain size should be 1/7 of the upper box height.

The surface of the exhumed materials had dust and dirt. Therefore, before taking the scanning electron microscopy images the samples were cleaned, avoiding additional damage. More details on this process were presented by Pinho-Lopes and Lopes 2013.

2.2 Materials

2.2.1 Geosynthetics

This paper includes results for two geosynthetics (Table 3 and Figure 3): a woven geotextile (GTX), consisting of polypropylene (PP) tapes; and a coated yarn geogrid (GGR), consisting of high tenacity polyester (PET) yarns covered with black polymeric coating woven into a grid structure. The nominal tensile strength of the geosynthetics in the machine direction was 65kN/m and 55kN/m, respectively, for GTX and GGR. The mass per unit area of GTX was 320g/m^2; the openings of GGR were 18mm x 18mm and the thickness ranged between 1.5mm and 2.3mm (Figure 3b). As some samples of GTX were stolen from the construction site, there was less material available for testing.

The tensile properties of the geosynthetics, determined using wide-width tensile tests (BSI 2008, EN ISO 10319) were: tensile strength 77.5kN/m and strain at break 13% for GTX; and tensile strength 83.4kN/m and strain at break 15% for GGR. The tensile strength measured was significantly higher than the nominal values presented by the producers of the geosynthetics.

2.2.2 Soils

A different soil (soil S1 or soil S2) was used in each field trial, each compacted to two different energies (CE1 and CE2).. Due to site issues and storing constraints in the laboratory, soil S1 and S2 were not available to perform the pullout and the inclined plane shear tests. However, two other soils, S3 and S4, from adjacent construction sites, were identified as sufficiently similar to soils S1 and S2, respectively. The materials had the same origin and types of particles, as well as similar particle size distributions. Due to scale limitations in the inclined plane shear test, the larger particles (>10mm) of soil S3 had to be removed and the resulting soil was designated by soil $S3_{10}$. Figure 4 and Table 4 include additional information on the soils. Table 5 summarises further properties of soils S3, S4 and $S3_{10}$, relevant for interpreting the soil-geosynthetic interaction tests.

The soil relative density adopted for the tests (I_D=50%) was chosen to avoid additional damage on the geosynthetics associated with the tests set-up, particularly due to spreading, levelling and compacting the soil. Additionally, such conditions were chosen to represent areas near the facing of reinforced soil structures where often the compaction of the soil is not very easy to achieve without inducing additional loads on the facing system.

The test program (Table 1) includes assessing the soil-geosynthetic interface response in pullout and inclined plane shear of undamaged (UND) samples, used as a reference, and exhumed samples. As two different confining soils were considered, the undamaged samples were tested separately with each of those soils (3 specimens per confining soil).

3 RESULTS AND DISCUSSION

3.1 Scanning electron microscopy observations

The surface of the geosynthetics was affected by the installation damage (Figure 5). GTX exhibits lamination of its constituent tapes, some puncturing and fibre cutting. Installation damage tended to affect the coating of GGR, as well as the fibres underneath. Fibre cutting was also observed. The visually observed consequences of installation damage were particularly important for the most severe installation conditions (ID S1 CE2).

3.2 Pullout tests

Undamaged and exhumed samples (submitted to installation damage with either soil S1 or soil S2) of the two geosynthetics were confined in soils S3 or S4, respectively, and tested for pullout. The confining stress at the geosynthetic was 13kPa for soil S3 and 50kPa for soil S4. The different values were a consequence of changes implemented on the equipment between the two sets of tests. The results from the pullout tests are summarized in Table 6 and include the mean values for the maximum pullout force (P_{max}), the peak frontal displacement (d_f) and the secant stiffness for 50% of P_{max} (J_{50}), the corresponding coefficients of variation (COV, in %) and the failure mode observed for three (valid) specimens (BSI 2004, EN 13738). The dimensions of the samples tested were: for GTX, 0.25m x 0.75m for samples tested in soil S3 and 0.30m x 1.00m, for samples tested in soil S4; GGR, ~0.316m (15 ribs) x ~1.050m (50 ribs). Previously cut samples (with smaller dimensions) forced using smaller specimens of GTX confined in soils S3. The ratios between the minimum GGR aperture and the average soil particle size of soils S3 and S4 were 0.43 and 3.85, respectively. The particles of soil S4 were smaller than the minimum aperture dimension of the grid, thus enabling the soil particles to enter those apertures. However, about 15% of the particles of soil S3 were larger than the apertures of GGR.

When confined in soil S3 both GTX and GGR failed in tensile (mostly in their unconfined section), while in soil S4 only pullout failures were observed. The true pullout strength of the interfaces exhibiting tensile failures will be higher than the maximum pullout force measured during the test. The latter force is lower than the corresponding tensile strength measured due to different griping conditions and test speeds: tensile tests - both ends of the geosynthetic are fixed in clamps, strain rate ~20mm/min; pullout tests - one end is fixed in a clamp, imposed displacement rate 2mm/min. Similar trends were reported by Pinho-Lopes et al. (2015) for two extruded geogrids. Nevertheless, for some samples similar reductions of the maximum forces measured in tensile tests (presented by Paula et al. (2008)) and in pullout tests were found (for example, ~9% for GTX ID S1 CE1 and ~40% for GGR S1 CE1).

The installation damage changed the pullout response of both GTX and GGR (Figures 6 and 7). When tested for pullout confined in soil S3 after exhumation from soil S1 both geosynthetics exhibited a reduction of the maximum pullout force, relatively to the intact sample tested under similar conditions. For the samples confined in soil S4 after exhumation from soil S2 (pullout failures) a different trend was observed: GTX exhibited reductions of the maximum pullout force, while GGR had increased pullout forces (between 2%, for ID S2 CE2, and 10%, for ID S2 CE1). After installation damage all samples tested exhibited a reduction of stiffness during the pullout tests (illustrated in Figures 6a and 7a). This is likely to be a consequence of the response on the unconfined length of the specimens. The secant stiffness for 50% of the maximum pullout force, J_{50}, represents the response of the soil-geosynthetic interface for small displacements, when compared to those associated with the maximum pullout force. The changes in J_{50} after exhumation (Table 6) showed that when confined in soil S4 (pullout failures) the reductions in stiffness of the soil-geosynthetic interfaces studied were more important than those of the pullout strength. For the tensile failures an opposite trend was observed.

For GTX (Figure 6b) the length of the specimens mobilized at failure was not always the same. This was particularly relevant for the specimens of GTX confined in soil S3. Some of those specimens were not completely mobilized (although the specimens were shorter than those confined in soil S4). This seems to indicate that using short specimens did not affect the results obtained. The previously induced damage reduced the mobilized length at failure of the specimens of GTX confined in soil S3. That reduction was higher for the most severe installation conditions (ID S1 CE2). The premature tensile failure (in its unconfined section) prevented the geotextile to be mobilized along all the available length. Oppositely, when confined in soil S4 and for pullout failures, the complete length of GTX specimens was contributing to the strength mobilized. Regardless of the type of sample, the unconfined section of the geosynthetics underwent significant deformations, as illustrated by the steep slopes of the initial part of the curves in Figures 6b and 7b for x<0mm (corresponding to the metal sleeve).

The displacement relative to the end of the specimen along the reinforcement length provides information on the stress transfer from the soil to the reinforcement. Thus, Figures 6b and 7b give some indication on the mobilisation of shear stresses on the soil-reinforcement interface.

3.2.1 Coefficient of interaction in pullout

The soil-geosynthetic interface strength is often characterized using coefficients of interaction. Although the mobilized strength along a reinforcement during pullout is different (for example, the peak strength is mobilized in some areas and the constant volume strength in others), average values of the coefficient of interaction can be determined. Lower estimates of such values can be obtained using Equation 1, where: τ_p, maximum shear stress mobilized on the soil-geosynthetic interface during the pullout test (Equation 2); τ_s, maximum shear stress obtained from direct shear tests of the same soil for the same normal stress; P_{max}, maximum pullout force mobilized per unit width; L, confined length of the reinforcement when the maximum pullout force per unit width is mobilized.

$$f = \frac{\tau_p}{\tau_s} \quad (1)$$

$$\tau_p = \frac{P_{max}}{2L} \quad (2)$$

For specimens exhibiting pullout failures the coefficient of interaction should be within the range of f_{LR} and f_{Le}, determined, respectively, using the total confined length of the reinforcement for the maximum pullout force ($L=L_R$) and the effective confined length for the maximum pullout force ($L=L_e$). The forces mobilized along the geosynthetic can be determined (for example using the method by Ochiai et al. 1996). However, such method requires using the load-strain response of the geosynthetics obtained from in-isolation tensile tests performed at the same speed as the pullout tests (often not available).

The soil-geosynthetic coefficients of interaction were determined (Equation 1) using either the confined length for the maximum pullout force (L_R) or the effective length for the maximum pullout force (L_e). These led to the coefficient of interaction identified as f_{LR} and f_{Le}, respectively, determined using mean values for all specimens tested (Table 7). For specimens exhibiting pullout failures the coefficient of interaction should be within the range of f_{LR} and f_{Le}. Some values of f are larger than 1.0, which is not likely to occur (particularly for sheet materials like GTX).

The coefficient of interaction estimated for interfaces with soil S3 needs to be analysed carefully, as those values correspond to tensile failures. If when confined in soil S3 the geosynthetics were strong enough to avoid the tensile failures two consequences, with opposite effects on the coefficient of interaction, would be expected: on the one hand, the measured pullout force would increase; while, on the other hand, the length of geosynthetic mobilized would also increase. Therefore, depending on the relative values of the changes in P_{max} and L, the coefficient of interaction would also be expected to be lower than the values extimated from the tensile values (presented in Table 7).

GTX is a sheet and skin friction is the only mechanism mobilising soil-geosynthetic interface strength. The damage induced in the field tests seems to have reduced such strength for samples installed in soil S1 (which exhibited premature tensile failures) and for the sample installed in soil S2 (pullout failures). For both cases, it is likely that the pullout forces transmitted to the geosynthetic along its unconfined section had to arch around damaged areas, generating stress concentrations which then led to earlier failure (particularly tensile).

For GGR besides skin friction, the soil-geosynthetic interface strength also depends on the soil-soil friction mobilized along its openings and passive thrust on its transverse ribs, depending on the relative movement occurring. Samples confined in soil S4 exhibited increased pullout resistance after installation damage. On the one hand, it is likely that the damage induced helped creating a rougher surface; on the other hand, the detachment of fibres and coating observed may have contributed to a localized higher thickness of the bearing members (thus mobilizing more passive thrust).

The coefficient of interaction between the two soils and GGR determined using Equation 1 is an approximation considering the geogrid as an equivalent uniform and continuous sheet. To estimate the contribution of the bearing members some approaches available in the literature have been used. According to Jewell (1996), the coefficient of interaction soil-geogrid in pullout (f) can obtained from Equation 3, where: f_{sf}, and f_{bm} are, respectively, the contributions of the skin friction and of the bearing members to the coefficient of interaction; a_s is the fraction of the geogrid surface area that is solid (available to mobilize friction), δ is the friction angle at the soil-reinforcement interface, ϕ' is the soil friction angle in terms of effective stresses, $\left(\frac{\sigma'_p}{\sigma'_n}\right)_\infty$ is the bearing stress mobilized when the soil particle size is unimportant, a_b is the fraction of the width of the geogrid available for bearing, B is the thickness of the geogrid bearing members and S is the distance between bearing members. Factors F_1 (Equation 4) and F_2 (Equation 5) allow for the influence of the soil particle size and the shape of the bearing members of the grid, respectively. These factors were proposed by Palmeira and Milligan (1989) based on results from pullout tests performed with metallic grids confined in sand. For the interface between sands and extensible materials, such as extruded geogrids, factor F_1 (Equation 4) was found too optimistic (Lopes and Lopes 1999b). Lopes and Lopes (1999a) reported contributions of the bearing members of extruded geogrids for the pullout strength confined in two different sands of ~ 26%.

$$f = f_{sf} + F_1 F_2 f_{bm} = a_s \frac{\tan\delta}{\tan\phi'} + F_1 F_2 \left(\frac{\sigma'_p}{\sigma'_n}\right)_\infty \frac{a_b B}{S} \frac{1}{2\tan\phi'} \tag{3}$$

$$\begin{aligned} &F_1 = \left(2 - \frac{B}{10D_{50}}\right) \; when \; \frac{B}{10D_{50}} < 10 \\ &F_1 = 1 \; when \; \frac{B}{10D_{50}} \geq 10 \end{aligned} \tag{4}$$

$$\begin{aligned} &F_2 = 1 \; for\ circular\ bars \\ &F_1 = 1.2 \; for\ rectangular\ bars \end{aligned} \tag{5}$$

Equation 6 represents the bearing stress mobilized when the soil particle size is unimportant, for soils without cohesion (as summarized by Lopes, 2012) and is the lower bound for the passive resistance mobilized on bearing members of a grid (adopting the shear failure mechanism by puncture on deep foundations for soils). Equation 7 represents the upper bound of the bearing stress mobilized, for soils without cohesion. Table 8 includes values of f_{bm}, using these lower (Equation 6) and the upper (Equation 7) bound estimates (f_{bm}^- and f_{bm}^+, respectively), with and without using factors F_1 and F_2. As these equations are applicable to soils without cohesion, for soil S3 two sets of estimates are presented, for values of ϕ' determined with and without cohesion.

$$\left(\frac{\sigma'_p}{\sigma'_n}\right)_\infty = tan\left(\frac{\pi}{4} + \frac{\phi'}{2}\right) e^{\left(\frac{\pi}{2} + \phi'\right) tan\,\phi'} \tag{6}$$

$$\left(\frac{\sigma'_p}{\sigma'_n}\right)_\infty = tan^2\left(\frac{\pi}{4} + \frac{\phi'}{2}\right) e^{\pi\, tan\,\phi'} \tag{7}$$

The estimates for the contribution of the bearing members are very high (in most cases >1.0), particularly when the corrections F_1 and F_2 are included. These results seem to corroborate the conclusions by Lopes and Lopes (1999b). On the one hand, the equations were developed for metallic grids (much stiffer than extensible reinforcements). On the other hand, GGR has a woven structure and, therefore, it is likely that some bearing members move relatively to the adjacent longitudinal bars when submitted to passive thrust. Such movement contributes to reducing the contribution of the bearing members. When the tests were disassembled this type of movement was observed (Figure 8).

The results from the pullout tests for samples confined in soils S3 and S4 can be compared using the values of the coefficient of interaction, as these represent the interface strength normalized to the shear strength of the soil. Nevertheless, there are two significant constraints to this comparison: 1) the failure mode observed was different, thus the true pullout strength in soil S3 was not determined; 2) the normal stress applied at the geosynthetic was not the same (13 kPa for S3 and 50 kPa for S4). For the first constraint, the results for tensile failures are low estimates of the pullout strength, indicating that the trend observed may be even more important. For the second constraint, increasing the normal stress applied to a geosynthetic confined in a soil will increase the pullout strength. The results presented (Table 7) showed that the highest confining stress led to the lowest coefficient of interaction, as the coefficient of interaction with soil S3 was larger than with soil S4 (except for GTX ID S1 CE2). This seems to indicate that using soil S3 instead of soil S4 to confine the geosynthetics tested had more impact on the results than the corresponding normal stresses. A previous paper (Pinho-Lopes et al. 2015) reported similar conclusions, in which three other geosynthetics with a grid structure (two extruded geogrids and a grid composite) were studied.

3.3 Inclined plane shear tests

Table 9 summarizes the results from the inclined plane shear tests between each geosynthetic and soils $S3_{10}$ and S4. Table 9 includes mean values for the angle of friction of the soil-geosynthetic interface (δ_{sg}), the inclination angle for initiation of the sliding of the upper box (β_d) and the displacement of the upper box for which the sudden sliding of the upper box initiates (d_S), as represented in Figure 9. Table 9 also includes the coefficients of variation (COV, in %) for the different properties calculated. Representative displacement versus inclination graphs are summarized in Figures 10 and 11, for GTX and GGR, respectively.

The angle of friction of the soil-geosynthetic interface (δ_{sg}) of the exhumed samples was smaller, when compared to the corresponding value for the undamaged material (except for GGR ID S1 CE2). As before, the strength mobilized on the soil-GTX interface is skin friction.

Therefore the results seem to indicate that after installation the contact surface of GTX was smoother. After exhumation the samples were covered with dust and some fine soil particles. As the samples were not cleaned before testing, such surface layer may have contributed to the reduction of the interface friction measured.

For GGR, a similar reduction of the angle of friction was observed after installation in soil S2 and in soil S1 CE1. However, after installation of GGR in soil S1 compacted to CE2 the angle of friction of the soil-geosynthetic interface increased relatively to the undamaged sample. GGR was tested with a lower box with soil. Thus soil-soil friction is mobilized along the apertures of the geogrid, as well as skin friction along its surface. As after damage the dimension of the apertures did not change and the soil in contact with the geogrid was always the same, the differences observed are likely to be caused by different mobilisation of skin friction. The reduction of adherence in the interface with GGR may have been caused by the accumulation of fine particles previously mentioned for GTX. After exhumation from soil S1 CE2 (the most severe installation conditions) the surface of GGR was particularly damaged (the coating was partial removed, exposing the undulated surface of the fibres; many fibres were cut and damaged), which may have contributed to a rougher surface and less significant accumulation of fine particles.

From the results, particularly the coefficient of variation for the interface angle of friction, the repeatability of the results was found adequate. The coefficient of variation for δ_{sg} is lower than 2.8% for most samples; the highest values correspond to GTX, undamaged (5.9%) and exhumed from soil S1 CE1 (4.1%). Nevertheless, when the sliding process is analysed (using the values of β_d and d_S), the scatter of responses found was important (coefficient of variation between 6% and 17% for β_d and 4% and 43% for d_S). This seems to indicate that the sliding process can vary significantly. It was not possible to confirm if a similar trend has been observed by other authors because not enough relevant information was found in the literature.

A gradual sliding process was observed for GTX (Figure 10) and for most samples of GGR (Figure 11). Two specimens of GGR ID S1 CE2 had some degree of stick-slip response during the transitory phase. The stick-slip response may be caused by localized areas of rougher surface, as observed after installation in soil S1 CE2. It is likely that when that localized higher skin friction was mobilized the specimens exhibited a sudden displacement, until another area with similar features was fully mobilized.

3.3.1 Coefficient of interaction in inclined plane shear

The coefficient of interaction between the geosynthetics and soils $S3_{10}$ and S4 in inclined plane shear (f_{ips}) are presented in Table 9. For the same soil and installation conditions, the coefficient of interface with GTX was lower than that with GGR. The soil-soil shear strength mobilized on the geogrid apertures is the main reason for such differences. The angle of friction of soil $S3_{10}$ was higher than that of soil S4 (Table 5). Although ~12% of soil $S3_{10}$ particles were larger than the apertures of GGR, most particles entered those apertures and enabled mobilising soil-soil strength. All particles of soil S4 were smaller than the geogrid openings. The installation damage induced in the field trials had little influence on the coefficient of interaction between soil and geosynthetic in inclined plane shear. The most affected interface was GTX-soil $S3_{10}$, due to the changes observed on the surface of the geotextile (namely the accumulation of fines).

3.4 Coefficient of interaction in pullout and in inclined plane shear

Although performed for different vertical stresses, the test results allow comparing the coefficient of interaction between each geosynthetic with soil S4 for the two types of movement analysed (pullout and inclined plane shear). The coefficients of interaction obtained for samples in contact with soil S4 using pullout tests were always lower than those obtained from the inclined plane shear tests (Tables 7 and 9). There are several causes for such differences.

For GTX, during the inclined plane shear tests the reinforcement was fixed to a rigid base and the soil above the geotextile was free to move, mobilising skin friction along all the contact area. During the pullout test the geosynthetic moved relatively to the surrounding soil (above and below). Thus, skin friction was mobilized on both upper and lower surfaces of the reinforcement. However, the geotextile also deformed and was displaced (when all its length was mobilized). The largest movements associated with the pullout test caused lower mobilisation of interface strength.

For GGR the surface area available for mobilising skin friction was smaller than for GTX. Additionally, as the geogrid was displaced in the pullout tests, passive thrust could be progressively mobilized against the geogrid bearing members. During the inclined plane shear tests (using a lower box filled with soil and GGR fixed on its top) there was relative movement of the two soil layers (above and below the geogrid) enabling mobilization of soil-soil shear strength.

3.5 Reduction factor for installation damage

Traditionally the reduction factor for installation damage is computed by comparing the tensile strength of an undamaged sample of a geosynthetic with that measured after field installation. In this paper such reduction factor was identified as $RF_{ID\ tensile}$ (Equation 8), where $T_{max\ UND}$ and $T_{max\ DAM}$ are, respectively, mean values of the tensile strength of undamaged and exhumed samples. These results (presented by Paula et al. (2008)) refer to 5 specimens per sample tested according to BSI (2008) EN ISO 10319. From the tests results relevant reduction factors for installation damage were calculated (Figure 12). Using the pullout response the reduction factor $RF_{ID\ pullout}$ (Equation 9) was calculated comparing mean values of the maximum pullout forces of undamaged and damaged samples ($P_{max\ UND}$ and $P_{max\ DAM}$) tested under the same conditions (same confining soil). The reduction factor for installation damage obtained from the inclined plane shear tests, $RF_{ID\ ips}$ (Equation 10), was computed as the ratio between the coefficient of friction soil - undamaged geosynthetic ($\tan \delta_{sg\ UND}$) and that of soil – damaged geosynthetic ($\tan \delta_{sg\ DAM}$). The minimum value for the reduction factors is 1.0. In some cases this threshold was not met, due to an increase of the mean value of the relevant property after exhumation.

$$RF_{ID\ tensile} = \frac{T_{\max UND}}{T_{\max DAM}} \tag{8}$$

$$RF_{ID\ pullout} = \frac{P_{\max UND}}{P_{\max DAM}} \tag{9}$$

$$RF_{ID\ ips} = \frac{\tan \delta_{sg\ UND}}{\tan \delta_{sg\ DAM}} \tag{10}$$

The samples tested for pullout confined in soil S3 exhibited tensile failures. Therefore, their true pullout strength was not measured and the corresponding values presented in Figure 12 are upper limits of the reduction factors for installation damage for such sets of conditions. The reduction factor for installation damage for GTX exhumed from soil S1 calculated using pullout data was smaller than that using data from tensile tests. If the true pullout strength had been assessed such difference could increase. For GGR $RF_{ID\ pullout}$ was larger than $RF_{ID\ tensile}$. As the $RF_{ID\ pullout}$ values presented are upper limits of the real reduction factor, this relationship may not be valid. Due to the scale issues in the inclined plane shear test and the need to use soil $S3_{10}$ as an alternative to soil S3, a direct comparison between the corresponding values of $RF_{ID\ ips}$ and $RF_{ID\ pullout}$ was not possible.

For the samples confined in soil S4 all results are directly comparable. For GTX the reduction factors obtained from the tensile tests and the pullout tests data are identical (1.10) and the $RF_{ID\ ips}$ is close to the threshold (1.01). For GGR the reduction in strength measured in the tensile tests was higher than that of the soil-geosynthetic interface either in pullout (represented by $RF_{ID\ pullout}$) or in inclined plane shear ($RF_{ID\ ips}$). For GGR the lowest reduction factor was obtained in the pullout tests (below 1.0).

Thus, for these geosynthetics and the conditions considered in the tests, the pullout strength (for pullout failures only) was little affected by the construction and installation processes ($RI_{ID\ pullout}$ ranging between 0.91 and 1.10). For GGR the $RF_{ID\ tensile}$ was an overestimate of the strength reduction observed for the soil-geogrid interface (similarly to what was reported by Pinho-Lopes et al. 2015 for other geogrids). When comparing the reduction factors obtained using the soil-geosynthetic interface properties the trend depended on the type of geosynthetic. For GTX $RF_{ID\ ips}$ was the lowest, while for GGR the opposite occurred.

4 CONCLUSIONS

In this paper the behaviour of two geosynthetics in pullout and inclined plane shear was investigated, after exhumation from field installation trials. From the results the main conclusions are:

- Installation damage can induce premature tensile failures in pullout tests, along the unconfined section of geosynthetics. For materials where this response was observed, a significant reduction of the coefficient of interaction between soil and geosynthetic could be found.
- As on site the soils are compacted with some moisture (usually related to the optimum water content), installation processes can cause the accumulation of a layer of fine particles over the geosynthetics. For backfill materials with a fine fraction, this phenomenon can be very important. Such layer is likely to reduce the skin friction available. Therefore, for sheet reinforcements in which fine particles can become trapped, some reduction in interface strength may be expected after installation, not necessarily due to damage of the geosynthetic.
- The estimates of the contribution of GGR bearing members to the coefficient of interface in pullout were very high. The equations used were developed for metallic grids. Additionally, the junctions of GGR allow for relative movement between longitudinal and transverse ribs, alleviating the stresses mobilized in the bearing members.
- The installation damage induced in the field trials had little influence on the coefficient of interaction between soil and geosynthetic in inclined plane shear. The most affect

interface was GTX-soil $S3_{10}$, due to the changes observed on the surface of the geotextile (namely the accumulation of fines).

- The different relative movements of soil and geosynthetic occurring during pullout and inclined-plane shear tests, as well as the deformation of the reinforcements during pullout, enable different mobilization of the interface strength. For the comparable conditions tested, the coefficient of interaction from inclined plane shear tests was larger than that measured using pullout tests, regardless of the geosynthetic structure.
- The reduction factor for installation damage obtained from tensile tests overestimated the effects of the installation conditions on the soil-geosynthetic interface from both pullout and inclined plane shear tests.

NOTATION

Basic SI units are given in parentheses.

a_b	fraction of the width of the geogrid available for bearing (-)
a_s	fraction of the geogrid surface area that is solid (available to mobilize friction) (-)
B	thickness of the geogrid bearing members (m)
c'	Drained cohesion (Pa)
d_f	Frontal displacement for the maximum pullout force (m)
D_{max}	Maximum soil particle size (m)
d_s	Displacement of the upper box in the inclined-plane shear test for which the sudden movement of the box occurs (m)
D_x	Largest particle size in the smallest x% of the soil particles (m)
F_1	Factor for influence of the soil particle size (-)
F_2	Factor for influence of the shape of the bearing members of the grid (-)
f	Soil-geosynthetic coefficient of interaction (-)

f_{bm}	Contribution of the bearing members to the soil-geosynthetic coefficient of interaction of grids (-)
f_{ips}	Soil-geosynthetic coefficient of interaction in inclined-plane shear (-)
f_{Le}	Soil-geosynthetic coefficient of interaction in pullout for the effective confined length of the reinforcement (-)
f_{LR}	Soil-geosynthetic coefficient of interaction in pullout for the confined length of the reinforcement (-)
f_{sf}	Contribution of the skin friction to the soil-geosynthetic coefficient of interaction of grids (-)
I_D	Soil relative density (%)
J_{50}	Secant stiffness for 50% of the maximum pullout force (N/m)
L	Confined length of the reinforcement when the maximum pullout force is mobilized (m)
L_0	Initial confined length of the reinforcement (m)
L_e	Effective confined length of the reinforcement when the maximum pullout force is mobilized (m)
L_R	Confined length of the reinforcement when the maximum pullout force is mobilized (m)
P_{max}	Maximum pullout force (N/m)
$P_{max\ DAM}$	Mean value of the maximum pullout force of the damaged sample (N/m)

$P_{max\ UND}$	Mean value of the maximum pullout force of the undamaged sample (N/m)
$RF_{ID\ ips}$	Reduction factor for installation damage obtained from the inclined plane shear tests (-)
$RF_{ID\ pullout}$	Reduction factor for installation damage obtained from the pullout tests (-)
$RF_{ID\ tensile}$	Reduction factor for installation damage obtained from the tensile tests (-)
S	distance between bearing members (m)
$T_{max\ DAM}$	Mean value of the tensile strength of the damaged sample (N/m)
$T_{max\ UND}$	Mean value of the tensile strength of the undamaged sample (N/m)
w_{opt}	Optimum water content (%)
x	Position along the geosynthetic plane in the pullout test (m)
β	Inclination of the upper box in the inclined-plane shear tests, relatively to the horizontal (°)
β_0	Inclination angle of the upper box in the inclined-plane shear tests, relatively to the horizontal, at the static limit equilibrium (°)
β_{50}	Inclination angle of the upper box in the inclined-plane shear tests, relatively to the horizontal, to a displacement of 50mm (°)
β_d	Inclination angle for initiation of the sliding of the upper box in the inclined-plane shear tests, relatively to the horizontal (°)

β_s	Inclination angle of the upper box in the inclined-plane shear tests, relatively to the horizontal, for non-stabilized sliding (°)
δ_{sg}	Angle of friction for the soil-geosynthetic interface (°)
$\delta_{sg\ DAM}$	Mean value of the angle of friction for the soil-geosynthetic interface for damaged samples (°)
$\delta_{sg\ UND}$	Mean value of the angle of friction for the soil-geosynthetic interface for undamaged samples (°)
ϕ'	Drained friction angle (º)
γ	Soil unit weight (N/m^3)
γ_{dmax}	Maximum dry unit weight (N/m^3)
γ_{max}	Maximum unit weight (N/m^3)
γ_{min}	Minimum unit weight (N/m^3)
σ_n	Normal stress at the geosynthetic (Pa)
τ_p	Maximum shear stress mobilized on the soil-geosynthetic interface during the pullout tests (Pa)
τ_s	Maximum shear stress obtained from direct shear tests of the soil (Pa)
COV	Coefficient of variation
CE	Compaction energy
GGR	Geogrid
GTX	Geotextile
ID	Installation damage

S	Soil
UND	Undamaged
PET	Polyester
PP	Polypropylene
RF_{ID}	Reduction factor for installation damage

ACKNOWLEDGEMENTS

The authors would like to thank the financial support of FCT (Fundação para a Ciência e para a Tecnologia) - Portugal, Research Project PTDC/ECM/099087/2008 and COMPETE, Research Project FCOMP-01-0124-FEDER-009724.

REFERENCES

AASHTO (2011) M 288-06:2011 Standard Specification for Geotextile Specification for Highway Applications. American Association of State Highway and Transportation Officials, USA.

Abdi MR and Zandieh AR (2014) Experimental and numerical analysis of large scale pull out tests conducted on clays reinforced with geogrids encapsulated with coarse material. *Geotextiles and Geomembranes* 42(5): 494–504.

Allen TM and Bathurst RJ (1994) Characterization of geosynthetic load-strain behavior after installation damage. *Geosynthetics International* 1(2): 181-199.

Allen TM and Bathurst RJ (1996) Combined allowable strength reduction factor for geosynthetic creep and installation damage. *Geosynthetics International* 3(3): 407-439.

ASTM (2000) D698-00a: Standard Test Methods for Laboratory Compaction Characteristics of Soil Using Standard Effort (12,400 ft-lbf/ft^3 (600 kN-m/m^3)). ASTM International, West Conshohocken, PA, USA.

Austin RA (1998) Installation effects on geosynthetics. Seminar volume on Installation Damage in Geosynthetics, November 1998, ERA Technology, Leatherhead, U.K., pp. 3.2.1-3.2.10.

Bathurst RJ, Huang B and Allen TA (2011) Analysis of installation damage tests for LRFD calibration of reinforced soil structures. Geotextiles and Geomembranes 29(3): 323-334.

Bathurst RJ and Miyata Y (2015) Reliability-based analysis of combined installation damage and creep for the tensile rupture limit state of geogrid reinforcement in Japan. *Soils and Foundations* 55(2): 437–446.

Briançon L, Girard H and Gourc JP (2011) A new procedure for measuring geosynthetic friction with an inclined plane. *Geotextiles and Geomembranes* 29 (5): 472-482.

BSI (2004) EN 13738:2004. Geotextiles and geotextile-related products - Determination of pullout resistance in soil. BSI, London, UK.

BSI (2005) EN ISO 12957-2:2005. Geosynthetics - Determination of friction characteristics -- Part 2: Inclined plane test. BSI, London, UK.

BSI (2007) EN ISO/TR 20432:2007: Guidelines to the determination of long-term strength of geosynthetics for soil reinforcement. BSI, London, UK.

BSI (2008) EN ISO 10319:2008: Geosynthetics. Wide-width tensile test. BSI, London, UK.

Chen C, McDowell GR and Thom NH (2014) Investigating geogrid-reinforced ballast: Experimental pullout tests and discrete element modelling. *Soils and Foundations* 54(1): 1-11.

Cho SD, Lee KW, Cazzuffi DA and Jeon HY (2006) Evaluation of combination effects of installation damage and creep behavior on long-term design strength of geogrids. *Polymer Testing* 25(6): 819-828.

Ezzein FM and Bathurst RJ (2014) A new approach to evaluate soil-geosynthetic interaction using a novel pullout test apparatus and transparent granular soil. *Geotextiles and Geomembranes* 42(3): 246–255.

FGSV (2005) Merkblatt über die Anwendung von Geokunststoffen im Erdbau des Straßenbaues, FGS Koln, Germany.

Gourc JP and Reyes Ramirez R (2004) Dynamics-based interpretation of the interface friction test at the inclined plane. *Geosynthetics International* 11(6): 439-454.

Greenwood JH (2002) The effect of installation damage on the long-term design strength of a reinforcing geosynthetic. *Geosynthetics International* 9(3): 247-258.

Greenwood JH, Schroeder HF and Voskamp W (2012) Durability of Geosynthetics. CUR Building & Infrastructure, Gouda, The Netherlands, Publication 243.

Huang C-C and Chiou S-L (2006) Investigation of installation damage of some geogrids using laboratory tests. *Geosynthetics International* 13(1): 23–35.

Huang C-C, Hsieh H-Y and Hsieh Y-L (2014) Hyperbolic models for a 2-D backfill and reinforcement pullout. *Geosynthetics International* 21(3): 168-178.

Huang C-C and Wang Z-H (2007) Installation damage of geogrids: influence of load intensity. *Geosynthetics International* 14(2): 65–75.

Hufenus R, Ruegger R, Flum D and Sterba IJ (2005) Strength reduction factors due to installation damage of reinforcing geosynthetics. *Geotextiles and Geomembranes* 23(5): 401-424.

Jewell RA, Milligan GWE, Sarsby RW and Dubois D (1984) Interaction between soil and geogrids. In Proceeding of Polymer Grid Reinforcement (Thomas Telford Ltd. Publisher), London, Great Britain, pp. 18-30.

Lajevardi SH, Briançon L and Dias D (2014) Experimental studies of the geosynthetic anchorage – Effect of geometric parameters and efficiency of anchorages. *Geotextiles and Geomembranes*, 42(5): 505-514.

Lim SY and McCartney JS (2013) Evaluation of effect of backfill particle size on installation damage reduction factors for geogrids. *Geosynthetics International* 20(2): 62–72.

Lopes ML (2012) Soil-geosynthetic interaction. In Handbook of *Geosynthetic Engineering, Geosynthetics and their applications* (Shukla SK (Ed)). ICE Publishing, Thomas Telford, London, UK, pp. 45-66

Lopes ML (2013) Friction at geosynthetic interfaces on inclined plane shear. *Indian Geotechnical Journal* 43 (4): 321-330.

Lopes ML and Ladeira M (1996) Influence of the Confinement, Soil Density and Displacement Rate on Soil-Geogrid Interaction. *Geotextiles and Geomembranes* 14: 543-554.

Lopes MJ and Lopes ML (1999a) Soil-geosynthetic interaction; influence of soil particles size and geosynthetic structure. *Geosynthetics International* 6(4): 261-282.

Lopes MP and Lopes ML (1999b) Mecanismos de interacção solo-geogrelhas – papel da granulometria do solo e das barras transversais do reforço. Geotecnia 87: 5-32 (*in Portuguese*).

Lopes PC, Lopes ML and Lopes MP (2001) Shear behaviour of geosynthetics in the inclined plane test – influence of soil particle size and geosynthetic structure. *Geosynthetics International* 8 (4): 327-342.

Miyata Y and Bathurst RJ (2015) Reliability analysis of geogrid installation damage test data in Japan. *Soils and Foundations* 55 (2): 393-403.

Ochiai H, Otani J, Hayashi S and Hirai T (1996) The pullout resistance of geogrids in reinforced soil. *Geotextiles and Geomembranes* 14(1): 19-42.

Palmeira EM (2009) Soil–geosynthetic interaction: Modelling and analysis. *Geotextiles and Geomembranes* 27 (5): 368-390.

Palmeira EM, Lima Jr NR and Mello LGR (2002) Interaction Between Soils and Geosynthetic Layers in Large-Scale Ramp Tests. *Geosynthetics International* 9(2): 149-187.

Palmeira EM and Milligan GWE (1989) Scale and other factors affecting the results of pull-out tests of grids buried in sand. Geotechnique 39(3):511-524.

Paula AM, Pinho-Lopes M and Lopes ML (2008) Combined effect of damage during installation and long-term mechanical behaviour of geosynthetics. paper 185, theme 3 (Durability and long term performance) of the 4th European Geosynthetics Conference, abstract book pp. 39, CD-ROM, 8p., Edinburgh, UK.

Pinho-Lopes M and Lopes ML (2013) Tensile properties of geosynthetics after installation damage. *Environmental Geotechnics* 1(3): 161-178.

Pinho-Lopes M, Paula M and Lopes ML (2015) Pullout response of geogrids after installation. *Geosynthetics International (in press)*

Pitanga HN, Gourc JP and Vilar OM (2009) Interface shear strength of geosynthetics: evaluation and analysis of inclined plane test. *Geotextiles and Geomembranes* 27(6): 435-446.

Tran VDH, Meguid MA and Chouinard LE (2013) A finite–discrete element framework for the 3D modeling of geogrid–soil interaction under pullout loading conditions. *Geotextiles and Geomembranes* 37: 1–9.

Wang Z, Jacobs F and Ziegler M (2014) Visualization of load transfer behaviour between geogrid and sand using PFC2D. *Geotextiles and Geomembranes* 42(2): 83-90.

Watn A and Chew SH (2002) Geosynthetic damage – from laboratory to field, in Proceedings of the 7th International Conference on Geosynthetics, Nice, France, Vol. 4, pp. 1203-1226.

Weerasekara L and Wijewickreme D (2010) An analytical method to predict the pullout response of geotextiles. *Geosynthetics International* 17(4): 193-206.

Zhou J, Chen J-F, Xue J-F and Wang J-Q (2012) Micro-mechanism of the interaction between sand and geogrid transverse ribs. *Geosynthetics International* 19(6): 426-437.

TABLES

Table 1 - Test program implemented and number of specimens tested.

Geosynthetic	Sample	Pullout (EN 13738)	Inclined plane shear (EN ISO 12957-2)
GTX	UND	6	6
	ID S1 CE1	3	3
	ID S1 CE2	3	3
	ID S2 CE2	3	3
GGR	UND	6	6
	ID S1 CE1	3	3
	ID S1 CE2	2	3
	ID S2 CE1	3	3
	ID S2 CE2	3	3

GTX – geotextile | GGR - geogrid

UND – undamaged | ID - installation damage | S - soil | CE - compaction energy

Table 2 – Characteristics of the compaction equipment used for the field damage trials (information presented previously in Pinho-Lopes and Lopes 2013).

Characteristic		Unit	Value
Weight	Operating weight CECE	kg	15600
	Operating weight (open cabin)		15200
	Linear	kg/m	43.9
	Loads - Front	kg	9000
	Loads - Back		6600
Cylinder dimensions	Width	mm	2100
	Diameter		1500
	Thickness		35
	Tires		23.1-26
Vibration	Amplitudes	mm	2.0/0.8
	Frequencies	Hz	28/38
	Centrifuge force	kN	280/220

Table 3 – Characteristics of the geosynthetics tested

Geosynthetic	Polymer	Mass per unit area (g/m^2)	Tensile strength (kN/m)	Strain at break (%)	Thickness (mm)	Grid openings (mm x mm)	Width of the ribs (mm)
GTX	PP	320	77.5	13.0	1.2	-	-
GGR	PET	-	83.4	14.9	1.5 to 2.3*	18 x 18*	4 - 5*

* More details are included in Figure 3b

Table 4 – Properties of soils (some data for soils S1 to S4 was previously presented in Pinho-Lopes et al. 2015)

Materials		Fines (%)	D_{10} (mm)	D_{30} (mm)	D_{50} (mm)	D_{60} (mm)	D_{max} (mm)	$\gamma_{dmax}^{\#}$ (kN/m^3)	$w_{opt}^{\#}$ (%)
S1	Crushed aggregate	5.18	0.22	2.68	11.78	19.15	50.80	20.7	7.80
S2	Residual soil of granite	21.53	0.07	0.17	0.38	0.68	5.00	18.8	11.30
S3	Crushed aggregate	9.52	0.08	1.00	3.50	5.95	37.50	20.3	7.0
S4	Residual soil of granite	19.87	-	0.19	0.39	0.55	38.10	18.8	10.5
$S3_{10}$	Crushed aggregate	3.63	-	1.00	2.67	3.67	10.00	20.7	8.5

$^{\#}$ - Standard Proctor (ASTM D 698-00a)

Table 5 – Additional properties of the soils used in the pullout and inclined plane shear tests (data for soils S3 and S4 was previously presented in Pinho-Lopes et al. 2015)

Materials		γ_{min} (kN/m^3)	$\gamma^{\#}$ (kN/m^3)	γ_{max} (kN/m^3)	$\phi'^{\#}$ (º)	$c'^{\#}$ (kPa)	
S3	Crushed aggregate	14.12	16.95	21.19	52.9	5.8	Peak
					50.9	5.2	Constant volume
S4	Residual soil of granite	13.59	15.18	17.20	41.1	0	Peak
					36.6	0	Constant volume
$S3_{10}$	Crushed aggregate	15.33	17.61	20.68	45.7	8.55	Peak
					42.5	8.49	Constant volume

$^{\#}$ - for a relative density I_D=50%

Table 6. Summary of the pullout tests results: mean values and coefficient of variation of maximum pullout force (P_{max}), the peak frontal displacement (d_f) and the secant stiffness for 50% of P_{max} (J_{50}), for undamaged and damaged samples.

Geosynthetic	Sample	σ_n (kPa)	Soil	γ^* (kN/m^3)	L_0 (m)	Failure mode (number of specimens)	P_{max} Mean (kN/m)	P_{max} COV$^+$ (%)	d_f Mean (mm)	d_f COV$^+$ (%)	J_{50} Mean (kN/m)	J_{50} COV$^+$ (%)
GTX	UND S1	13.3	S3	16.95	0.75	Tensile (3)	43.67	6.16	89.93	12.86	621.57	3.28
	ID S1 CE1					Tensile (3)	30.79	11.51	67.38	13.81	475.43	5.56
	ID S1 CE2					Tensile (3)	16.67	12.50	36.50	4.32	411.51	13.18
	UND S2	50	S4	15.18	1.00	Pullout (3)	47.13	6.57	108.98	5.19	485.88	6.29
	ID S2 CE2					Pullout (3)	43.02	5.02	119.53	5.98	409.03	6.36
GGR	UND S1	13.3	S3	16.95	1.05	Tensile (3)	48.43	6.14	84.30	9.11	724.51	1.56
	ID S1 CE1					Tensile (2)	29.10	7.65	74.31	9.83	525.70	15.90
	ID S1 CE2					Tensile (3)	20.31	35.12	44.84	16.66	607.95	16.31
	UND S2	50	S4	15.18		Pullout (3)	31.15	4.44	99.19	10.00	493.24	6.97
	ID S2 CE1					Pullout (3)	34.27	1.75	105.62	3.79	446.39	4.14
	ID S2 CE2					Pullout (3)	31.83	4.92	101.20	2.16	462.15	4.79

σ_n - normal stress at the geosynthetic | γ^* - unit weight of the soil, for I_D=50% | L_0 – initial confined length | COV$^+$ - coefficient of variation

Table 7. Stresses τ_s and τ_p and coefficient of interaction between soil and geosynthetic (f) from the pullout tests.

Geosynthetic	Sample	τ_s (kPa)	P_{max} (kN/m)	L_R (mm)	τ_p (kPa)	f_{LR} (-)	L_e (mm)	τ_p (kPa)	f_{Le} (-)	Failure mode (number of specimens)
GTX	UND S1	23.36	43.67	718.08	30.41	1.30	718.08	30.41	1.30	Tensile (3)
	ID S1 CE1	23.36	30.79	719.96	21.39	0.92	569.08	27.06	1.16	Tensile (3)
	ID S1 CE2	23.36	16.67	720.00	11.57	0.50	319.75	26.06	1.12	Tensile (3)
	UND S2	43.65	47.13	965.67	24.40	0.56	965.67	24.40	0.56	Pullout (3)
	ID S2 CE2	43.65	43.02	964.55	22.30	0.51	964.55	22.30	0.51	Pullout (3)
GGR	UND S1	23.36	48.43	1049.93	23.06	0.99	759.23	31.89	1.37	Tensile (3)
	ID S1 CE1	23.36	29.10	1049.93	13.86	0.59	759.69	19.16	0.82	Tensile (2)
	ID S1 CE2	23.36	20.31	1049.98	9.67	0.41	235.81	43.06	1.84	Tensile (3)
	UND S2	43.65	31.15	1046.83	14.88	0.34	1046.83	14.88	0.34	Pullout (3)
	ID S2 CE1	43.65	34.27	1046.75	16.37	0.38	1046.75	16.37	0.38	Pullout (3)
	ID S2 CE2	43.65	31.83	1048.34	15.18	0.35	1048.34	15.18	0.35	Pullout (3)

Table 8. Lower and upper bound for the passive resistance mobilized on the bearing members of GGR in pullout.

Soil	Strength parameters	c'	ϕ'	$(\sigma'_p/\sigma'_n)_\propto$	$(\sigma'_p/\sigma'_n)_\propto$	f_{bm}^-	f_{bm}^+	B/D_{50}	F_1	F_2	$F_1F_2f_{bm}^-$	$F_1F_2f_{bm}^+$
				(Eq. 6)	(Eq. 7)	(Eq. 3)	(Eq. 3)		(Eq. 4)	(Eq. 5)	(Eq. 3)	(Eq. 3)
		(kPa)	(°)	(-)	(-)	(-)	(-)	(-)	(-)	(-)	(-)	(-)
S3	Peak	5.76	52.92	80.95	568.42	2.06	14.48	0.429	1.96	1.20	4.84	34.01
	Constant volume	5.19	50.94	58.41	381.43	1.60	10.44	0.429	1.96	1.20	3.75	24.51
S4	Peak	0.00	41.12	16.22	75.15	0.63	2.90	3.846	1.62	1.20	1.21	5.63
	Constant volume	0.00	36.77	10.42	41.65	0.47	1.88	3.846	1.62	1.20	0.91	3.64
S3 (c'=0kPa)	Peak	0.00	54.89	115.26	870.97	2.73	20.65	0.429	1.96	1.20	6.42	48.49
	Constant volume	0.00	52.88	80.32	563.01	2.05	14.37	0.429	1.96	1.20	4.81	33.74

Table 9. Summary of the inclined plane shear tests results: mean values and coefficient of variation of the soil-geosynthetic interface friction angle (δ_{sg}), inclination angle for initiation of the sliding of the upper box (β_d) and displacement of the upper box for which the sudden sliding of the upper box initiates (d_S) and coefficient of interaction (f_{ips}), for undamaged and damaged samples.

Geosynthetic	Sample	Soil	γ^* (kN/m^3)	Test method	δ_{sg} Mean (°)	δ_{sg} COV$^+$ (%)	β_d Mean (°)	β_d COV$^+$ (-)	d_S Mean (mm)	d_S COV$^+$ (%)	f_{ips} (-)
GTX	UND S1	3_{10}	17.61	1	36.28	5.85	23.00	0.73	5.04	43.33	0.73
	ID S1 CE1				33.58	4.08	21.44	0.66	7.03	40.03	0.66
	ID S1 CE2				33.16	0.36	19.26	0.65	4.79	16.46	0.65
	UND S2	4	15.18		34.64	2.28	21.56	0.69	4.86	6.86	0.69
	ID S2 CE2				34.45	2.77	19.75	0.69	7.17	5.59	0.69
GGR	UND S1	3_{10}	17.61	2	38.11	0.98	23.44	0.78	9.07	18.85	0.78
	ID S1 CE1				37.93	1.94	23.86	0.78	8.99	8.31	0.78
	ID S1 CE2				38.40	1.49	25.26	0.79	8.67	14.53	0.79
	UND S2	4	15.18		36.18	2.27	22.18	0.73	13.34	16.32	0.73
	ID S2 CE1				35.90	0.67	20.82	0.72	13.37	3.50	0.72
	ID S2 CE2				35.60	2.78	16.89	0.72	15.47	12.49	0.72

γ^* - unit weight of the soil, for I_D=50% Test method: 1 – specimen on a rigid base; 2 – specimen on a lower box with soil

COV$^+$ - coefficient of variation

FIGURES

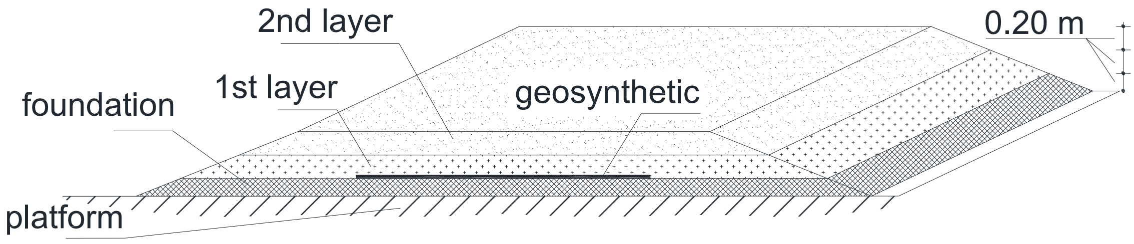

a)

b)

c)

Figure 1 – Field damage trials: a) cross section; b) compaction of a soil lift; c) manual exhumation of the samples.

a)

b)

Figure 2 – Equipment used for: a) pull-out tests; b) inclined plane shear tests.

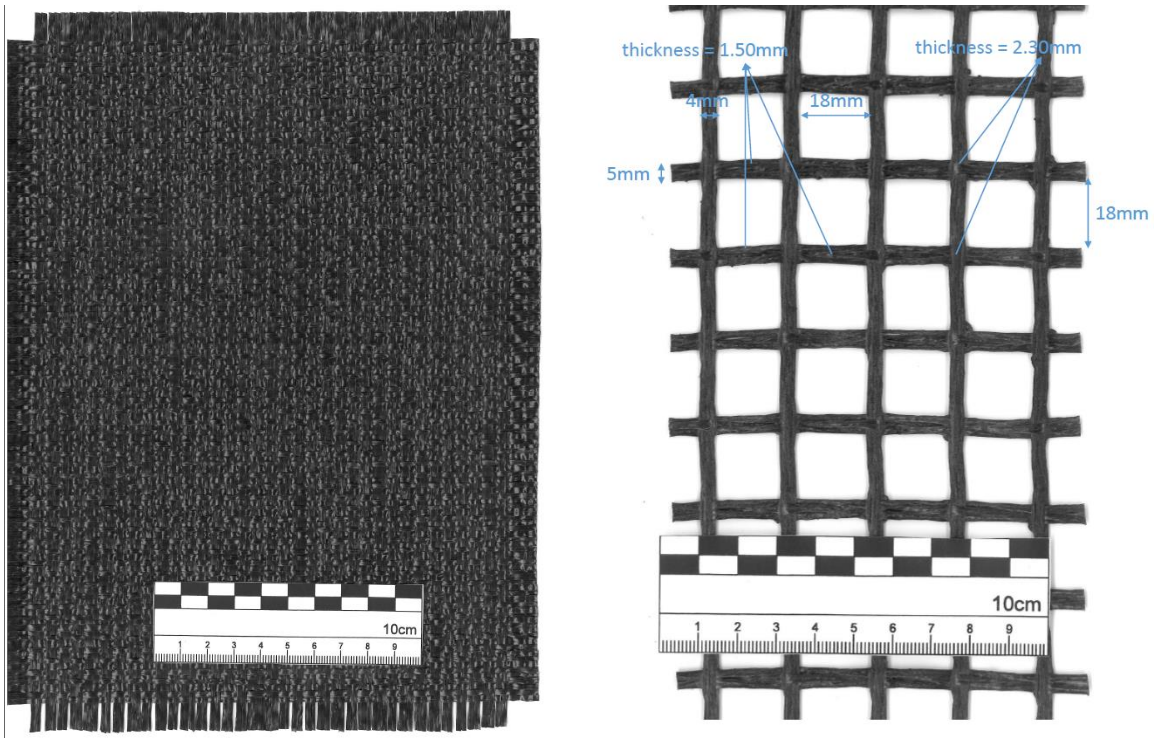

a) b)

Figure 3 – Geosynthetics tested: a) GTX; b) GGR.

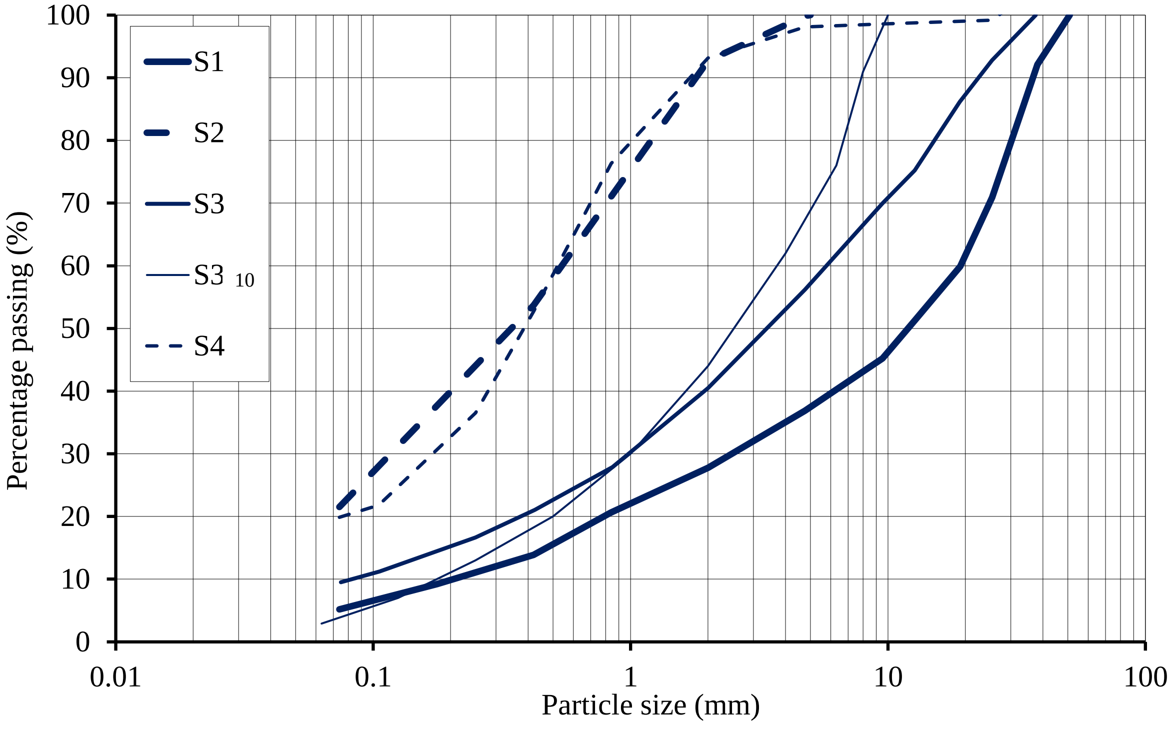

Figure 4 – Particle size distribution of the soils (data for soils S1, S2, S3 and S4 previously presented in Pinho-Lopes et al. 2015).

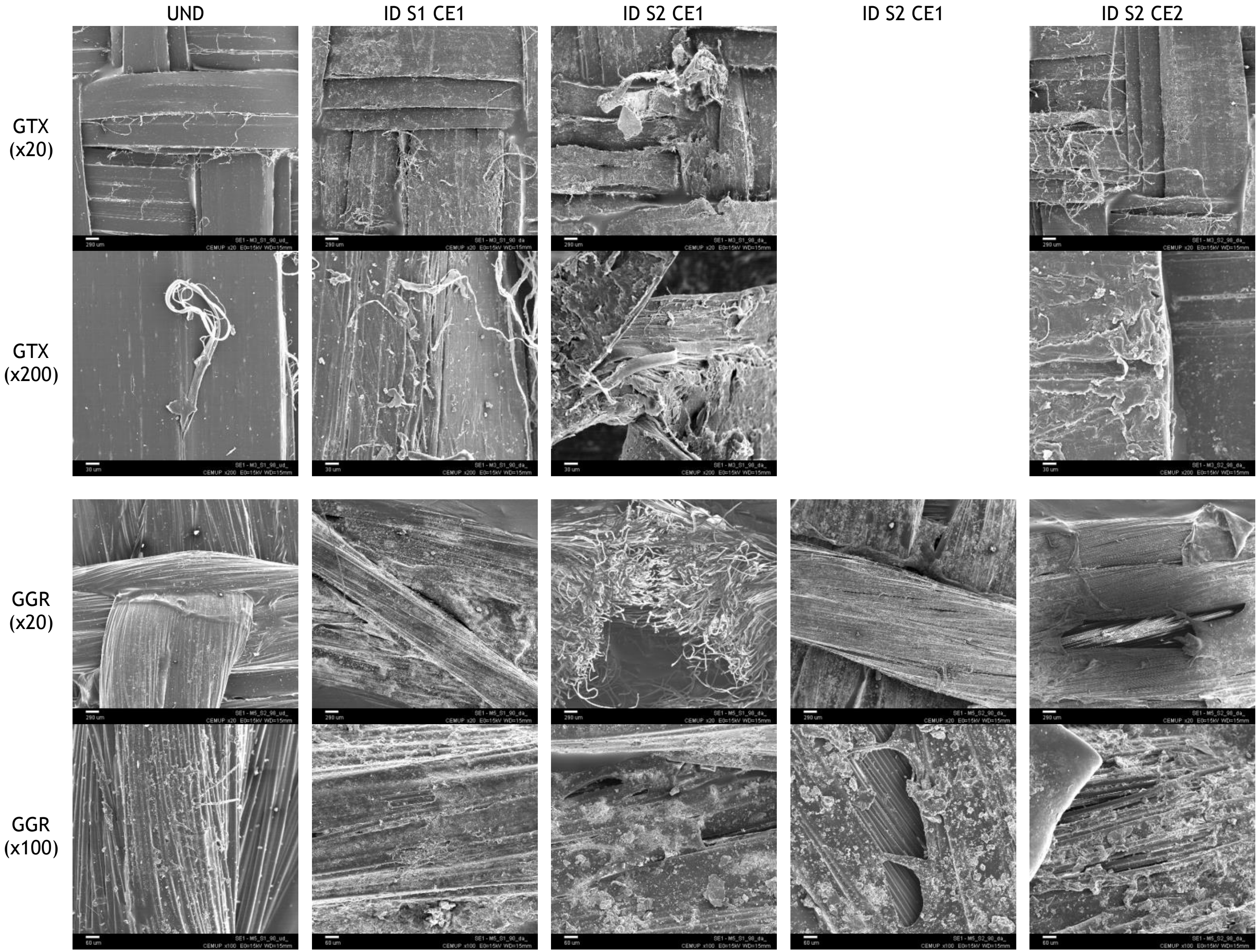

Figure 5 - Scanning electron microscopy images of GTX and GGR undamaged (UND), exhumed from soil S1 (ID S1 CE1, ID S1 CE1) and from soil S2 (ID S2 CE1, ID S2 CE2).

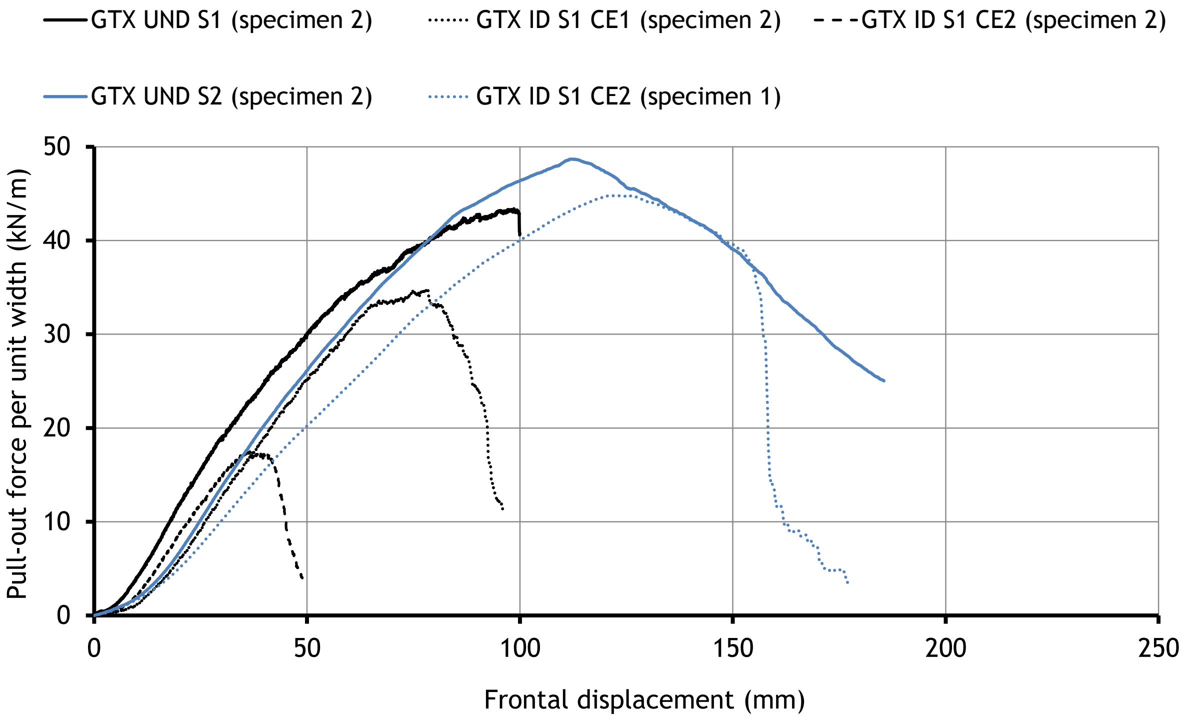

a)

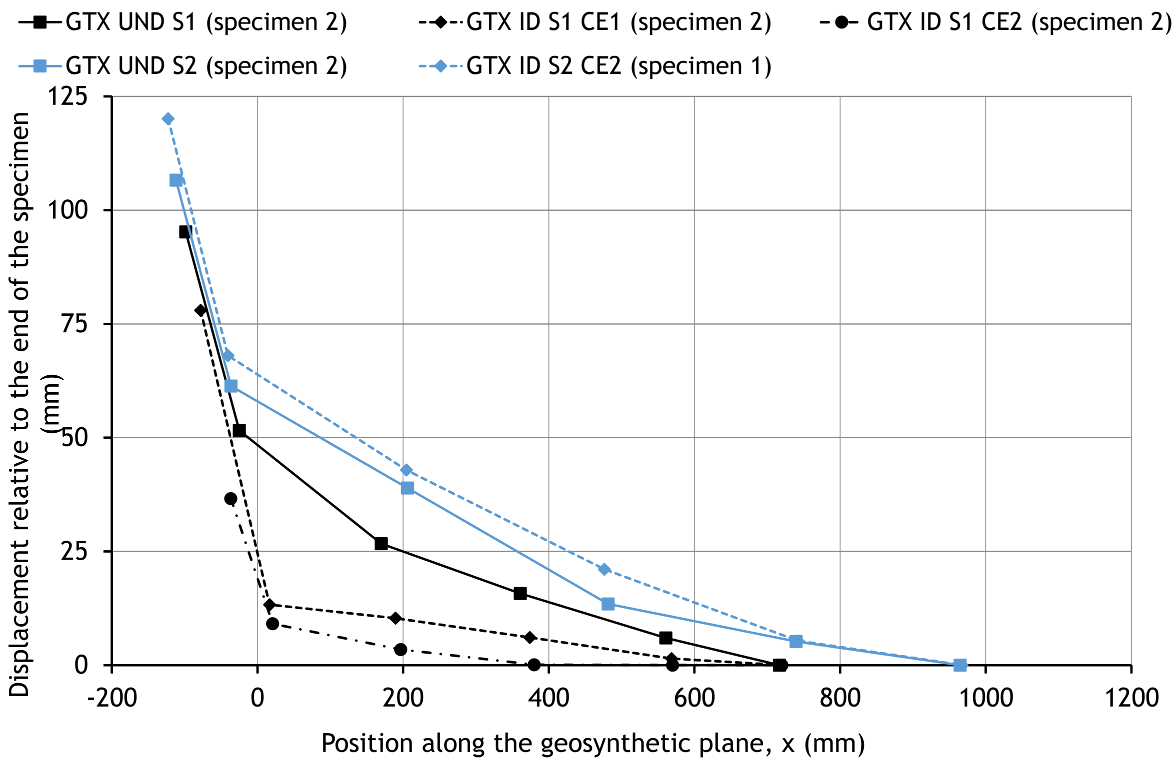

b)

Figure 6. Pullout response of GTX - one representative specimen per sample when confined in soil S3, σ_n=13.3 kPa (undamaged and after installation in soil S1), and in soil S4, σ_n=50 kPa (undamaged and after installation in soil S2): a) pullout force versus frontal displacement; b) displacements relatively to the end of the specimen, for the maximum pullout force, versus position along the geosynthetic plane (x<0mm refers to the unconfined area).

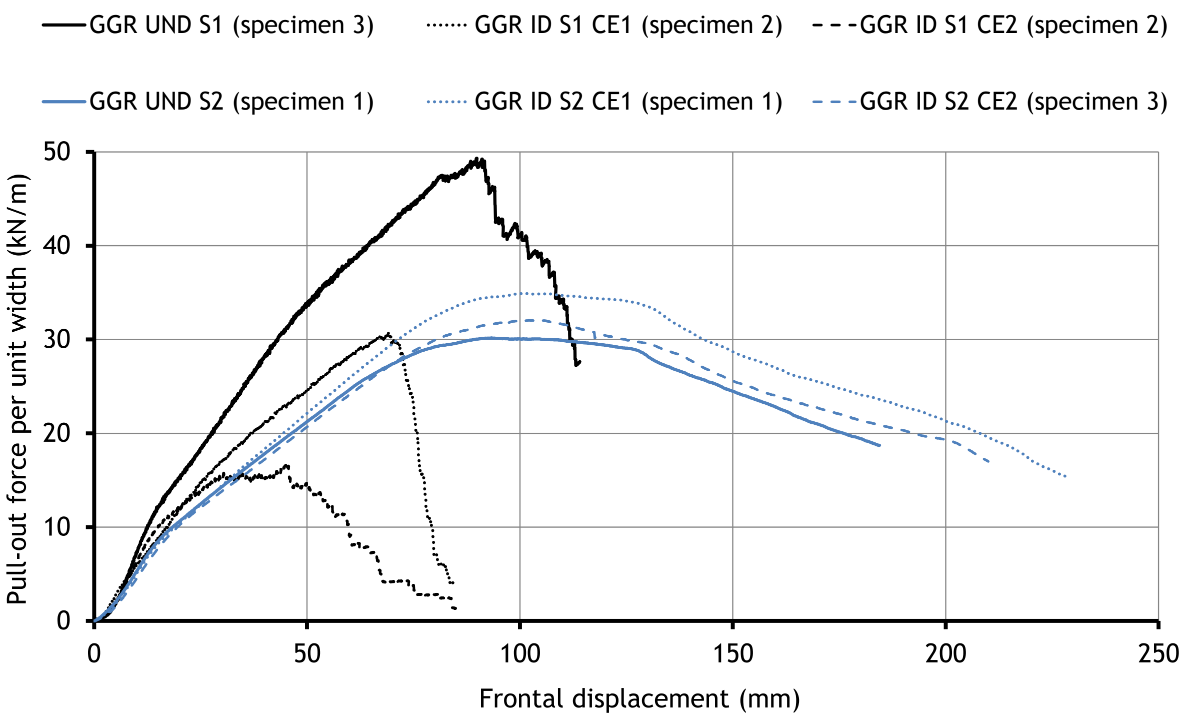

a)

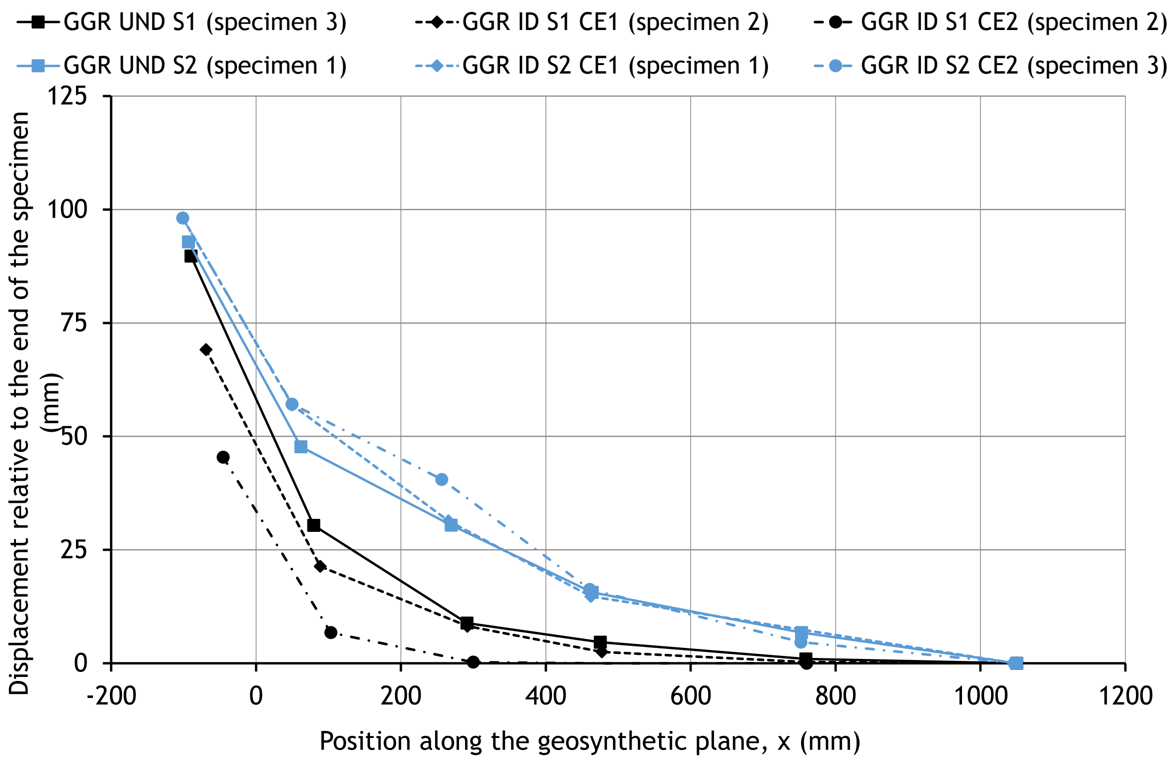

b)

Figure 7. Pullout response of GGR - one representative specimen per sample when confined in soil S3, σ_n=13.3 kPa (undamaged and after installation in soil S1), and in soil S4, σ_n=50 kPa (undamaged and after installation in soil S2): a) pullout force versus frontal displacement; b) displacements relatively to the end of the specimen, for the maximum pullout force, versus position along the geosynthetic plane (x<0mm refers to the unconfined area).

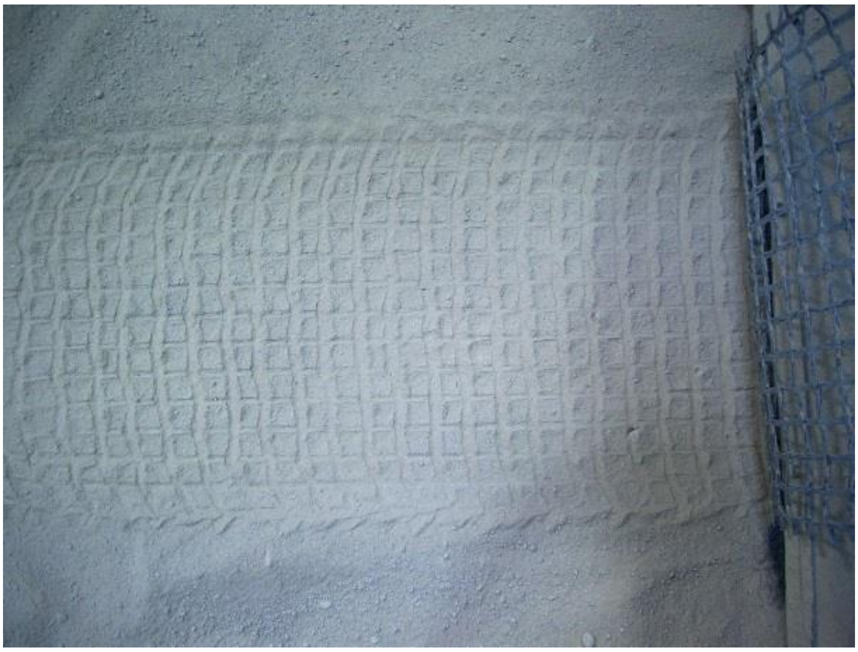

Figure 8. Negative of GGR in the confining soil (S4) after a pullout test.

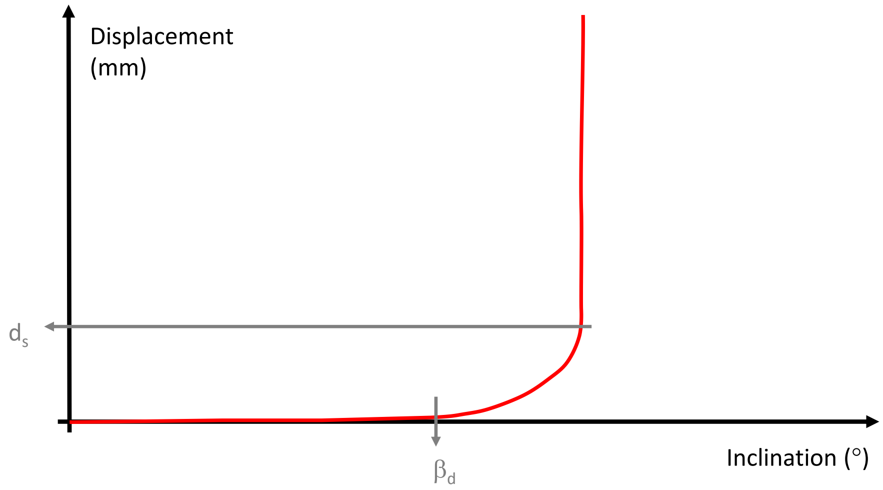

Figure 9. Schematic representation of parameters β_d and d_S, determined from the inclined plane shear tests results.

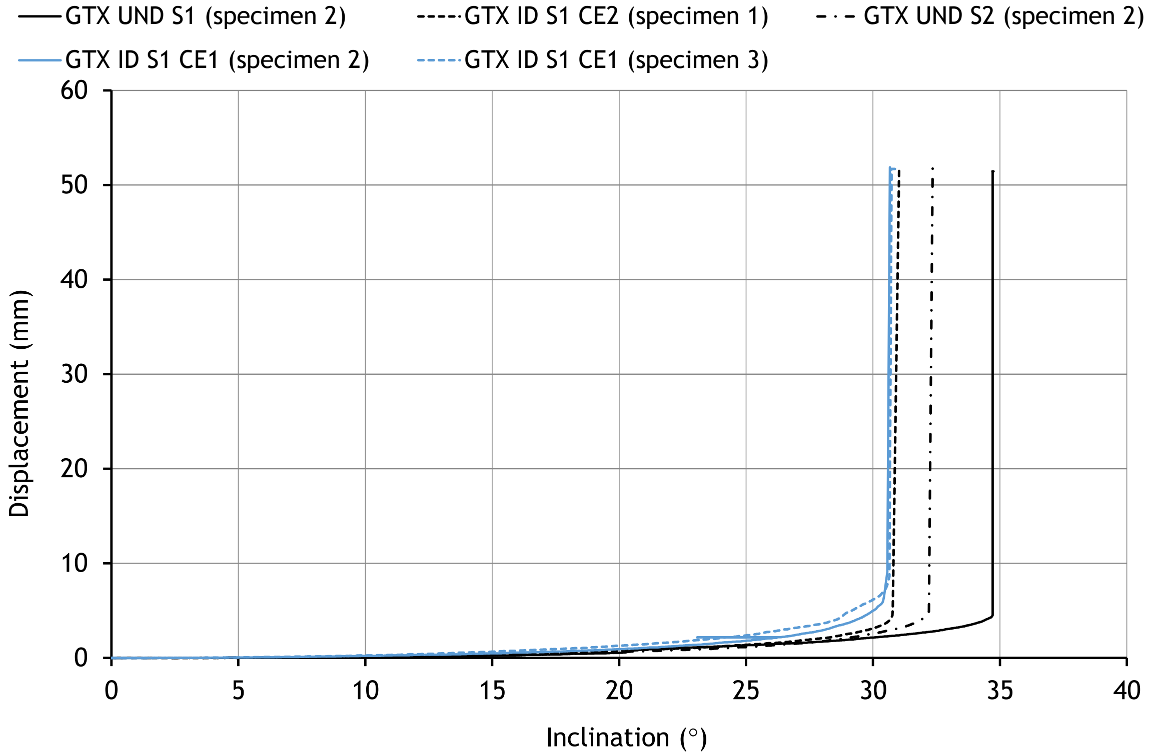

Figure 10. Inclined-shear plane response of GTX (displacement versus inclination curves for one representative specimen per sample) confined in soil $S3_{10}$ (undamaged and after installation in soil S1) and soil S4 (undamaged and after installation in soil S2).

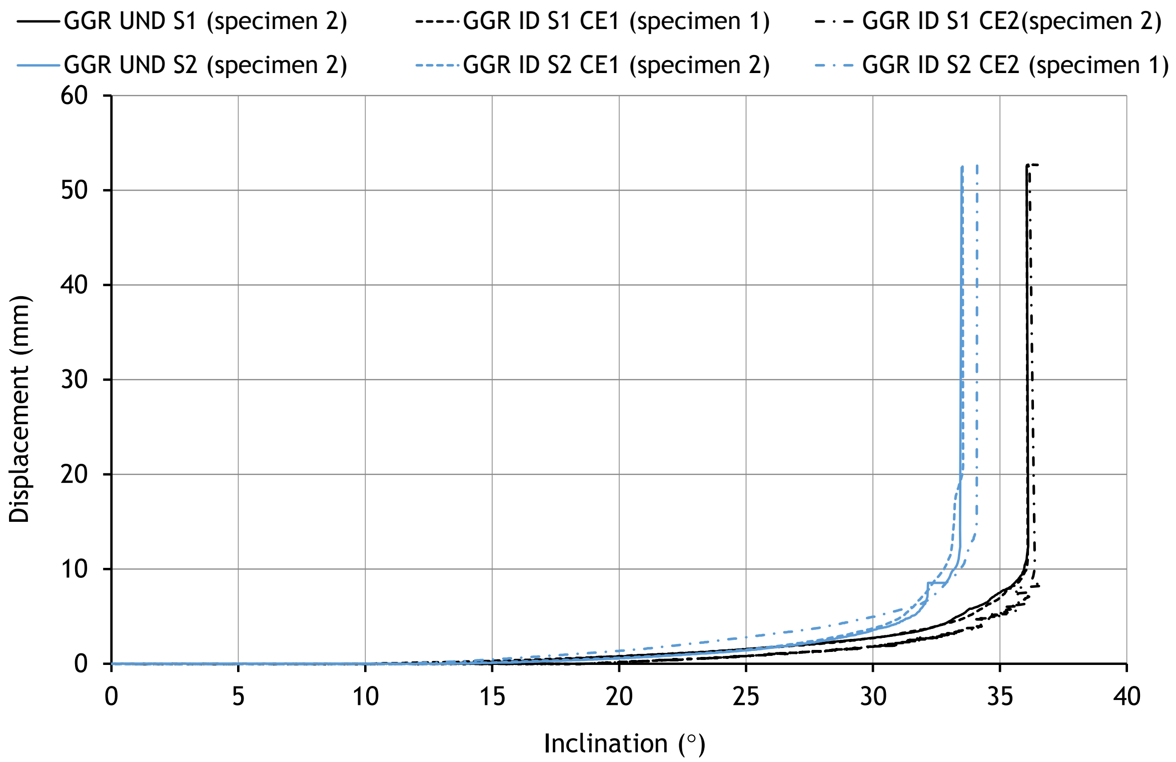

Figure 11. Inclined-shear plane response of GGR (displacement versus inclination curves for one representative specimen per sample) confined in soil S3$_{10}$ (undamaged and after installation in soil S1) and soil S4 (undamaged and after installation in soil S2).

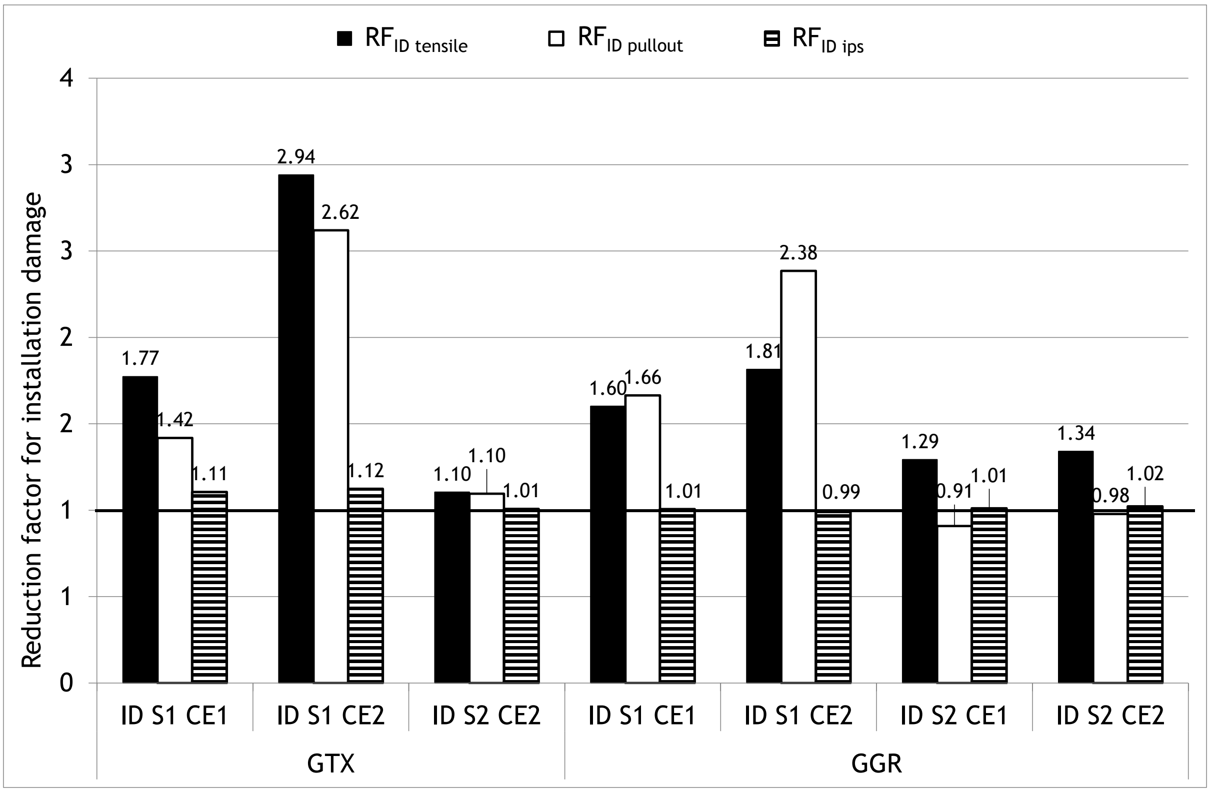

Figure 12. Reduction factors for installation damage of GTX and GGR after exhumation from the field damage tests obtained from different tests: wide-width tensile tests ($RF_{ID\ tensile}$); pullout tests ($RF_{ID\ pullout}$) and inclined plane shear tests ($RF_{ID\ ips}$).